Synthesis, structure and physical properties of the manganese(II) selenide/selenolate cluster complexes $[Mn_{32}Se_{14}(SePh)_{36}(PnPr_3)_4]$ and $[Na(benzene-15-crown-5)(C_4H_8O)_2]_2[Mn_8Se(SePh)_{16}]$†

Andreas Eichhöfer,*[a] Paul T. Wood,[b] Raghavan N. Viswanath[a] and Richard A. Mole[c]

Received (in Cambridge, UK) 21st September 2007, Accepted 21st January 2008
First published as an Advance Article on the web 12th February 2008
DOI: 10.1039/b714582a

The synthesis, molecular structures, and magnetic and optical properties of $[Mn_{32}Se_{14}(SePh)_{36}(PnPr_3)_4]$ and [Na(benzene-15-crown-5)$(C_4H_8O)_2]_2[Mn_8Se(SePh)_{16}]$ have been investigated which are the first examples of manganese chalcogenide cluster complexes, despite known manganese oxo compounds, which comprise more than four manganese atoms.

Metal chalcogenolato complexes have attracted interest due to their rich structural chemistry,[1] their potential use as precursors for M/Se materials[2] and their relevance as models for active sites of chalcogen-containing metalloproteins.[3] Since the discovery of single molecule magnet (SMM) behaviour in $[Mn_{12}O_{12}(O_2CCH_3)_{16}(H_2O)_4]\cdot 4H_2O\cdot 2CH_3CO_2H$,[4] manganese–oxo clusters have been one of the most active areas of study in molecular magnetism.[7] $[Mn_{84}O_{72}(O_2CMe)_{78}(OMe)_{24}(MeOH)_{12}(H_2O)_{42}(OH)_6]$[5] is the physically largest SMM, whilst $[Mn_{19}O_8(N_3)_8(MeC_6H_2O(CH_2O)_2H)_{12}(MeCN)_8]Cl_2$[6] has the largest ground state spin but is not a SMM. In comparison, molecules containing heavier chalcogens are much more limited in size,[8] with the largest containing only four Mn ions, *e.g.* $[Mn_4(SPh)_{10}]^{2-}$[8b] and $[Mn_4Te_4(TeiPr)_4]^{4-}$.[9] The most common route for synthesising these molecules is the reaction of MnX_2 with NaER (E = S, Se, Te).

According to Scheme 1, red crystals of $[Mn_{32}Se_{14}(SePh)_{36}(PnPr_3)_4]$ (**1**) were isolated from reaction solutions of $[Mn(SePh)_2]$ with 0.4 equivalents of $Se(SiMe_3)_2$ in the presence of $PnPr_3$. Reaction of $[Mn(SePh)_2]$ with 0.1 equivalents of $Se(SiMe_3)_2$ in the presence of NaSePh and benzene-15-crown-5 yielded the ionic compound [Na(benzene-15-crown-5)$(C_4H_8O)_2]_2[Mn_8Se(SePh)_{16}]$ (**2**).‡

1 crystallizes in the cubic space group *P*23 and exhibits a tetrahedral cluster core structure with four phosphine ligands at the apex positions (Fig. 1). The cluster framework is built up of 13 fused MnSe adamantanoid cages with four barrelenoid MnSe cages at each of the corners. Adamantanoid cages are the building blocks of the cubic zincblende structure of MnSe while barrelenoid cages are those of the hexagonal wurtzite type. Thus the structures are similar to the known M_{32} chalcogenide cluster molecules such as $[Cd_{32}S_{14}(SPh)_{36}(DMF)_4]$ (DMF = *N*,*N*-dimethylformamide),[10] $[Cd_{32}S_{14}(SCH_2CH(OH)CH_3)_{36}(H_2O)_4]$,[11] $[Hg_{32}Se_{14}(SePh)_{36}]$,[12] and $[Cd_{32}Se_{14}(SePh)_{36}(L)_4]$ (L = $OPPh_3$, OC_4H_8).[13] Bulk MnSe, however, normally crystallizes in the sodium chloride structure type.[14] All Mn atoms (Mn(1)–Mn(4)) have distorted tetrahedral coordination environments coordinated either solely by selenium atoms of $PhSe^-$ and Se^{2-} ligands (Mn(2)–Mn(3)) or three selenium atoms of $PhSe^-$ ligands and one phosphorus atom of the $PnPr_3$ ligands (Mn(1)) (Se–Mn–Se: 88.56(6)–122.41(8)°, P–Mn–Se: 104.36(7)°). The selenium atoms can be classified according to three different coordination modes: the Se^{2-} ligands display either a μ_4-bridging (Se(1) and Se(3)) or a μ_3-bridging (Se(2)) of the manganese atoms, whereas the $PhSe^-$ ligands are all μ_2-bridging. These differences in coordination mode and kind of ligand are mirrored in slightly different mean Mn–Se distances. μ_3-Se–Mn distances (249.4 pm) are on average found to be about 6 pm shorter than those for μ_4-Se–Mn (255.2 pm), whereas the latter are on the other hand about 2 pm shorter than the μ_2-PhSe–Mn bonding distances (256.9 pm). The interatomic distance in the four coordinated β-MnSe (zincblende modification) was found to be 254 pm.[15] The size of the resulting tetrahedral manganese selenide cluster can be best described by the edge lengths of 1875.4 pm of the tetrahedron formed by the four phosphorus atoms (P(1)) and the diameter of 1423.5 pm taken from Mn(1) at one vertex of the tetrahedron to the selenium atom ($Se(2^X)$) in the centre of the opposite tetrahedral face.

2 crystallizes in the monoclinic space group $P2_1/c$ and the molecular structure of the tetrahedral cluster anion

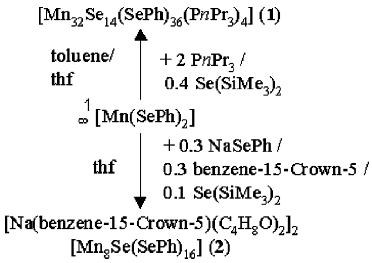

Scheme 1

---

[a] *Institut für Nanotechnologie, Forschungszentrum Karlsruhe, Postfach 3640, 76021 Karlsruhe, Germany. E-mail: eichhoefer@int.fzk.de; Fax: +49 7247-82-6368; Tel: +49 7247-82-6371*
[b] *University Chemical Laboratory, Lensfield Rd, Cambridge, UK CB2 1EW*
[c] *ZWE FRM-II, Lichtenbergstrasse 1, 85747 Garching, Germany*

† Electronic supplementary information (ESI) available: Synthesis, crystallography details, physical measurements, molecular structures, and temperature dependency graphs. CCDC 612695 and 612696. See DOI: 10.1039/b714582a.

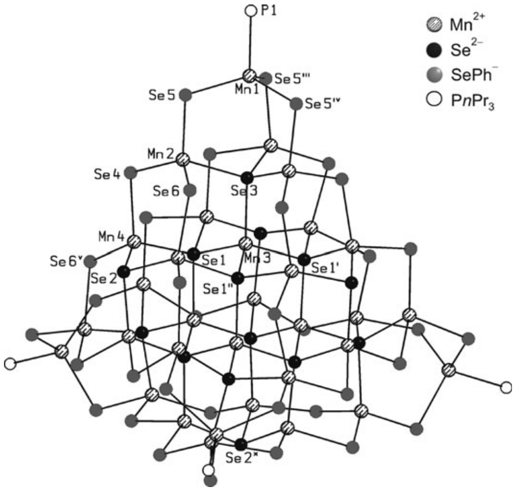

Fig. 1 The $Mn_{32}Se_{50}P_4$ cluster core as a section of the molecular structure of $[Mn_{32}Se_{14}(SePh)_{36}(PnPr_3)_4]$ (**1**). Symmetry transformation for generation of equivalent atoms: ^{I} $z + 1, -x + 1, -y$; ^{II} $y + 1, z, x - 1$; ^{III} $-z + 1, x - 1, -y$; ^{IV} $y + 1, -z, -x + 1$; ^{V} $z + 1, x - 1, y$; ^{X} $-x + 2, -y, z$.

$[Mn_8Se(SePh)_{16}]^{2-}$ is shown in Fig. 2. A central selenium atom Se(1) is tetrahedrally surrounded by four 'inner' manganese atoms Mn(1)–Mn(4). Each of these four inner manganese atoms are bound through three μ_2-PhSe$^-$ ligands Se(2)–Se(13) to one of the four 'outer' manganese atoms Mn(5)–Mn(8) which also form a tetrahedron. In addition, each of the four outer manganese atoms is bound to a terminal PhSe$^-$ ligand (Se(14)–Se(17)). All of the eight manganese atoms adopt a distorted tetrahedral coordination sphere (Se–Mn–Se: 99.33(5)–124.36(7)°). The selenium atoms form a distorted icosahedron with the eight manganese atoms bridging triangular faces, whereby four of the manganese atoms lie within and four outside of the icosahedron. The ranges of bond lengths are comparable to those found in **1**. In analogy to **1**, structurally related $M_8E(ER)_{12}$ (M = Zn, Cd; E = S, Se, Te; R = organic group) cluster cages are a well-known motif in group 12 metal chalcogenide cluster chemistry.[16]

UV-Vis spectra of rose-red crystals of **1** and **2** were measured in the solid state (nujol mull) (Fig. 3) and solution (thf) (see ESI†) which all display in principle similar features. The onset of the solid state absorption at roughly 575 nm is followed in both compounds by two overlapping absorption peaks with maxima around 487 and 466 nm and a weakly resolved shoulder at 430 nm. Similar two-peak structures have been observed in the absorption spectra of related cadmium and mercury chalcogenide cluster molecules and assigned to 4p → 5d ligand to metal charge transfer transitions due to their high extinction coefficients.[17] However, extinction coefficients around 600 M^{-1} cm^{-1} in **1** and 150 M^{-1} cm^{-1} in **2** suggest an assignment as spin forbidden but symmetry allowed d–d transitions in tetrahedrally coordinated manganese d^5 ions ($^4T_1(G) \leftarrow {}^6A_1$ 487 nm (20 534 cm^{-1}), $^4T_2(G) \leftarrow {}^6A_1$ 466 nm (21 459 cm^{-1}), $^4E(G) \leftarrow {}^6A_1$ 425 nm (23 529 cm^{-1})).[18] Further down, a broad absorption feature is detected as a shoulder in the solid state spectra around 310 nm, probably resulting from charge transfer transitions. This absorption is not well resolved in the solution spectra and most probably obscured by the tail of the next band around 244 nm which is very intense and originates from π–π* transitions of the PhSe$^-$ ligands. Interestingly, the absorption behaviours of both **1** and **2** are different to the structurally related Cd and Hg chalcogenide clusters where the absorption is shifted to higher wavelengths with increasing size.[17]

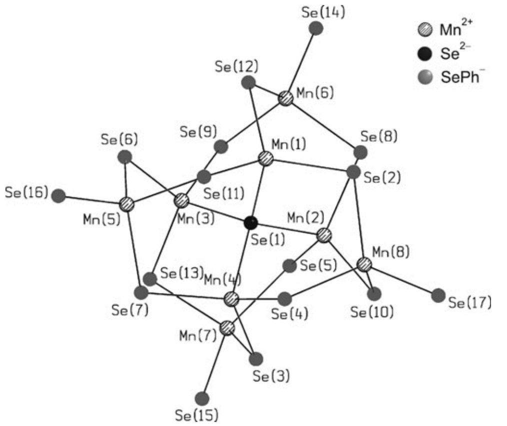

Fig. 2 The Mn_8Se_{17} cluster core as a section of the molecular structure of $[Na(benzene\text{-}15\text{-}crown\text{-}5)(C_4H_8O)_2]_2[Mn_8Se(SePh)_{16}]$ (**2**).

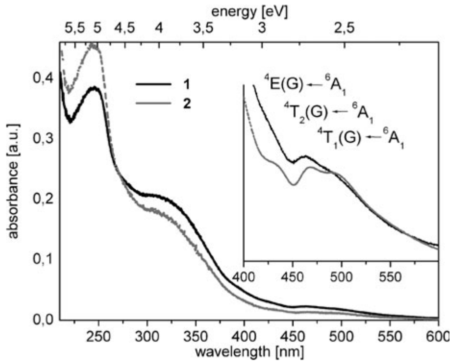

Fig. 3 UV-Vis spectra of $[Mn_{32}Se_{14}(SePh)_{36}(PnPr_3)_4]$ (**1**) and $[Na(benzene\text{-}15\text{-}crown\text{-}5)(C_4H_8O)_2]_2[Mn_8Se(SePh)_{16}]$ (**2**) in solid state (mull in nujol).

The susceptibilities of **1** and **2** were both measured in a field of 100 G. The graph of χT *versus* T for **1** decreases steadily with decreasing temperature and never reaches a saturation value at high temperature. This is in agreement with the large negative Weiss constant (−339(2) K) derived from a fit of the χ^{-1} *versus* T plot above 100 K, indicating strong antiferromagnetic interactions which is consistent with our recent findings on the magnetism of selenolate-bridged Mn(II) chains[19] and the work of Dehnen and co-workers.[20] The Curie constant (140.5 cm^3 mol^{-1} K) is in good agreement with the presence of 32 × $S = 5/2$ Mn(II). The AC susceptibility for **1** shows a maximum at 4 K with negligible frequency dependence which corresponds to the small plateau at low temperature in the DC data. There is no accompanying out-of-phase component as expected for an antiferromagnetic cluster with no possible source of zero-field splitting (*i.e.* isotropic metal ions in a rigorously tetrahedral cluster). Nevertheless, such high symmetry magnetic clusters have been shown to possess very unusual physical properties.[21] Compound **2** is potentially more interesting as, although it still contains the nominally isotropic Mn(II) ion, the symmetry of the cluster is much lower

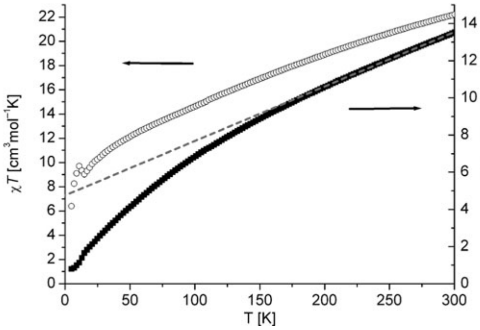

Fig. 4 χ^{-1} (filled square) and χT (open circle) *vs.* T plots measured at 100 G of [Na(benzene-15-crown-5)$(C_4H_8O)_2]_2[Mn_8Se(SePh)_{16}]$ (**2**). The dashed line represents the best fit obtained with a Curie–Weiss law above 200 K.

introducing the possibility of zero-field splitting. The magnetic topology of the cluster is a small tetrahedron encapsulated by a larger tetrahedron; however the cluster possesses only approximate 2-fold symmetry. It is therefore an all-Mn variant of the Mn_4Sn_4 clusters reported previously.[20b] The susceptibility increases steadily as the temperature is reduced going through a point of inflection at approximately 9 K, although it never reaches a plateau. Similar χT shows a gradual decrease with a small anomaly at low temperatures (Fig. 4). This data and the smaller Weiss constant of −162(2) K is consistent with weaker antiferromagnetic coupling than in **1**. The Curie constant derived from this fit of χ^{-1} *vs.* T plot above 200 K (34.2 cm^3 mol^{-1} K) is in reasonable agreement with 8 × S = 5/2 Mn(II). Isothermal magnetisation measurements at 2 K do not reach saturation at 9 T, but appear to be approaching a value of 10 μ_B mol^{-1}. Attempts were made to model this using the Hamiltonian $\hat{H} = D\hat{S}_z^2 + g_{iso}\mu_B SB$. The assumptions made in doing this are that the ground state is well isolated from any excited state at the specified temperature. This is a poor assumption for a system of eight Mn^{2+} ions. The frustration inherent in the topology will be relieved by inequivalent exchange pathways; hence the postulation of two uncompensated spins is not unreasonable. The degeneracy of the eleven S = 5 states will also be lifted by this distortion, as will the degeneracy of almost all other states. Consequently the existence of a low lying state of different S is highly likely. The AC susceptibility measured without additional static field shows a slow increase, followed by a very weakly field dependent maximum at approximately 2.2 K. There is no out of phase component to the susceptibility, indicating that any anisotropy is either very weak and thus not observable with these methods, or XY in nature.

Notes and references

‡ Synthesis of $[Mn_{32}Se_{14}(SePh)_{36}(PnPr_3)_4]$ (**1**): $Mn(SePh)_2$ (0.082 g (0.22 mmol)) was dissolved in 20 ml toluene upon addition of 9 ml of thf and $PnPr_3$ (0.18 ml, 0.89 mmol) to give an orange-brownish solution. $Se(SiMe_3)_2$ (0.023 ml (0.1 mmol)) was then added and the mixture stirred over night to give a light-red colour. After one week the solution was layered with diethyl ether to yield after another week red cubic crystals of **1**. Yield: 40%, 0.82 g. $C_{252}H_{264}Mn_{32}P_4Se_{50}$ (9122.8): calcd C 33.18, H 2.92; found C 33.2, H 2.9%. [Na(benzene-15-crown-5)$(C_4H_8O)_2]_2[Mn_8Se(SePh)_{16}]$ (**2**): $Mn(SePh)_2$ (0.112 g (0.31 mmol)) was dissolved in 20 ml thf to give an orange-brownish solution. A solution of NaSePh (0.012 g (0.09 mmol)) in 3.5 ml thf and a solution of benzene-15-crown-5 (0.025 g (0.09 mmol)) were then added and the mixture turned pale orange-red. The reaction solution was layered with diethyl ether two days after the addition of $Se(SiMe_3)_2$ (0.008 ml, 0.037 mmol) to give light-red crystals of **2**. Yield: 60%, 0.684 g. $C_{132}H_{136}Mn_8Na_2O_{12}Se_{17}$ (3742.3): calcd. C 42.37, H 3.66; found C 41.5, H 3.4%. Crystal data for **1**: $C_{252}H_{264}Mn_{32}P_4Se_{50}$, red cubic crystals, 0.12 × 0.1 × 0.1 mm, M_r = 9122.59, cubic, space group $P23$ (No. 195), $a = b = c$ = 2227.2(3) pm, V = 11 049(2) × 10^6 pm^3, Z = 1, D_c = 1.371 g cm^{-3}, μ(Mo-Kα) = 6.789 mm^{-1} giving a final $R1$ value of 0.0524 for 240 parameters and 3822 unique reflections with $I \geq 2\sigma(I)$ and w$R2$ of 0.1392 for all 15 661 reflections (R_{int} = 0.1002). For **2**: $C_{132}H_{136}Mn_8Na_2O_{12}Se_{17}\cdot 0.5C_4H_8O$, light-red prisms, 0.4 × 0.2 × 0.12 mm, M_r = 3778.28, monoclinic, space group $P2_1/c$ (No. 14), a = 2926.5(6), b = 2112.2(4), c = 2602.9(5) pm, β = 102.54(3)°, V = 15 705(5) × 10^6 pm^3, Z = 4, D_c = 1.598 g cm^{-3}, μ(Mo-Kα) = 4.617 mm^{-1} giving a final $R1$ value of 0.0681 for 1314 parameters, and 20 496 unique reflections with $I \geq 2\sigma(I)$ and w$R2$ of 0.2168 for all 96 176 reflections (R_{int} = 0.0692). CCDC 612695 (**1**) and 612696 (**2**). Temperature dependent DC susceptibilities were recorded on a Quantum Design MPMS-5S SQUID magnetometer on powdered samples sealed in evacuated quartz tubes.

1 I. Dance and K. Fisher, *Prog. Inorg. Chem.*, 1994, **41**, 637; S. Dehnen, A. Eichhöfer and D. Fenske, *Eur. J. Inorg. Chem.*, 2002, 279; M. W. DeGroot and J. F. Corrigan, in *Comprehensive Coordination Chemistry II*, ed. M. Fujita, A. Powell and C. Creutz, Pergamon, Oxford, UK, 2004, vol. 7, p. 57.

2 J. Arnold, *Prog. Inorg. Chem.*, 1995, **43**, 353; M. Bochmann, *Chem. Vap. Deposition*, 1996, **2**, 85.

3 B. Krebs and G. Henkel, *Angew. Chem.*, 1991, **103**, 785 (*Angew. Chem., Int. Ed. Engl.*, 1991, **30**, 769); B. Krebs and G. Henkel, *Chem. Rev.*, 2004, **104**(2), 801.

4 R. Sessoli, H.-K. Tsai, A. R. Schake, S. Wang, J. B. Vincent, K. Folting, D. Gatteschi, G. Cristou and D. N. Hendrickson, *J. Am. Chem. Soc.*, 1993, **115**, 1804.

5 A. J. Tasiopoulous, A. Vinslava, W. Wernsdorfer, K. A. Abboud and G. Christou, *Angew. Chem., Int. Ed.*, 2004, **43**, 2117.

6 A. M. Ako, I. J. Hewitt, V. Mereacre, R. Clerac, W. Wernsdorfer, C. E. Anson and A. K. Powell, *Angew. Chem., Int. Ed.*, 2006, **45**, 4926.

7 M. Manoli, A. Prescimone, R. Bagai, A. Mishra, M. Murugesu, S. Parsons, W. Wernsdorfer, G. Christou and E. K. Brechin, *Inorg. Chem.*, 2007, **46**, 6968; I. A. M. Pohl, L. G. Westin and M. Kritkos, *Chem.–Eur. J.*, 2001, **7**(16), 3439.

8 (*a*) T. Costa, J. Dorfman, K. S. Hagen and R. H. Holm, *Inorg. Chem.*, 1983, **22**, 4091; (*b*) W. Tremel, B. Krebs, K. Greiwe, W. Simon, H. Stephan and G. Henkel, *Z. Naturforsch., B: Chem. Sci.*, 1992, **47**, 1580; (*c*) H. Stephan, K. Griesar, W. Haase and G. Henkel, *Z. Naturforsch., B: Chem. Sci.*, 1994, **49**, 1620.

9 H.-O. Stephan, C. Chen, G. Henkel, K. Griesar and W. Haase, *J. Chem. Soc., Chem. Commun.*, 1993, 886.

10 N. Herron, J. C. Calabrese, W. E. Farneth and Y. Wang, *Science*, 1993, **259**, 1426.

11 T. Vossmeyer, G. Reck, L. Katsikas, E. T. K. Haupt, B. Schulz and H. Weller, *J. Am. Chem. Soc.*, 1995, **117**, 12881.

12 S. Behrens, M. Bettenhausen, A. C. Deveson, A. Eichhöfer, D. Fenske, A. Lohde and U. Woggon, *Angew. Chem.*, 1996, **108**, 2360–2363 (*Angew. Chem., Int. Ed. Engl.*, 1996, **35**, 2215).

13 A. Eichhöfer, *Eur. J. Inorg. Chem.*, 2005, 1245.

14 *Natl. Bur. Stand. Circ. (U.S.)*, 1960, **539**(10), 41.

15 R. M. Murray, B. C. Forbes and R. D. Heyding, *Can. J. Chem.*, 1972, **50**, 4059.

16 A. Eichhöfer, O. Hampe and M. Blom, *Eur. J. Inorg. Chem.*, 2003, 1307; G. S. H. Lee, K. J. Fisher, D. C. Craig, M. L. Scudder and I. G. Dance, *J. Am. Chem. Soc.*, 1990, **112**, 6435.

17 V. Soloviev, A. Eichhöfer, D. Fenske and U. Banin, *J. Am. Chem. Soc.*, 2000, **122**, 2673; V. Soloviev, A. Eichhöfer, D. Fenske and U. Banin, *J. Am. Chem. Soc.*, 2001, **123**, 2354; A. Eichhöfer and P. Deglmann, *Eur. J. Inorg. Chem.*, 2004, 349.

18 A. B. P. Lever, *Inorganic Electronic Spectroscopy*, Elsevier, Amsterdam, 2nd edn, 1984, p. 448.

19 A. Eichhöfer, P. T. Wood, R. Viswanath and R. A. Mole, *Eur. J. Inorg. Chem.*, 2007, 4794.

20 (*a*) M. Melullis, R. Clérac and S. Dehnen, *Chem. Commun.*, 2005, 6008; (*b*) M. K. Brandmayer, R. Clérac, F. Weigend and S. Dehnen, *Chem.–Eur. J.*, 2004, **10**, 5147.

21 S. Carretta, P. Santini, G. Amoretti, M. Affronte, A. Candini, A. Ghirri, L. S. Tidmarsh, R. H. Laye, R. Shaw and E. J. L. McInnes, *Phys. Rev. Lett.*, 2006, **97**, 207201.